

## Lessons from a time-dependent model

This article has been downloaded from IOPscience. Please scroll down to see the full text article.

1990 J. Phys. A: Math. Gen. 23 3953

(<http://iopscience.iop.org/0305-4470/23/17/025>)

View [the table of contents for this issue](#), or go to the [journal homepage](#) for more

Download details:

IP Address: 129.252.86.83

The article was downloaded on 01/06/2010 at 08:56

Please note that [terms and conditions apply](#).

# Lessons from a time-dependent model

Csaba Balázst

Central Research Institute for Physics, POB 49, H-1525 Budapest, Hungary

Received 31 March 1989, in final form 28 March 1990

**Abstract.** A particle is moving in an external field described by a stationary attractive potential and a time-dependent repulsive potential. It is shown that exact solutions of the time-dependent Schrödinger equation can be found for separable potentials. For a particle initially in a bound state the probability of remaining bound, and its energy spectrum in case it escapes, are calculated.

## 1. Introduction

In the present work a simple time-dependent model [1] will be applied and examined in some detail. A two-term potential is introduced which consists of an attractive time-independent part and of a repulsive, time-dependent part. In the beginning there is a bound state in the attractive potential. As one gradually strengthens the repulsion, the pole corresponding to the bound level moves towards the origin of the complex energy sheet and then becomes a resonant pole. We maintain the repulsion at a maximal level for a certain time, and then gradually switch it off. We are studying the dependence of the behaviour of a particle initially in a bound state on the parameters of our potential. Namely, we calculate the probability of staying in the bound state and the energy spectrum in case the particle escapes.

The potential is chosen to be separable, so we can solve the dynamical problem exactly. This is one of the most important features of our model, because there are very few methods to solve an explicitly time-dependent problem.

The model may have physical applications. The problem of a bound state becoming a quasistationary state might be related to heavy ion-heavy ion collisions and to laser-induced emission in atomic and solid state physics.

A further application may be the comparison of the method of separable potentials with the approximate methods for time-dependent external fields and for critical states.

## 2. Formulation

Let the Hamiltonian of a particle moving in a time-dependent external field be

$$\hat{H}(t) = \hat{H}_0 + \hat{V}(t) = \hat{H}_0 + \lambda_1 \hat{V}_1 + \lambda_2(t) \hat{V}_2 = \hat{H}_1 + \hat{V}_2(t) \quad (2.1)$$

† Present address: Department of Physics 009-00, Temple University, Philadelphia, PA 19122, USA.

‡ The formulation of the problem is based on [1], except for the shape of the time dependence of the Hamiltonian. In section 3 the idea of Révai to calculate the time-dependent states by solving a Volterra-type equation was also used.

where  $\hat{H}_0 = \hat{p}^2$  is the Hamiltonian of the free particle ( $\hbar = 2m = 1$ ). In (2.1) the external potential  $\hat{V}(t)$  consists of two parts,  $\hat{V}_1$  and  $\hat{V}_2$ , which are separable†:

$$\hat{V}_1 = |\beta_1\rangle\langle\beta_1| \quad \hat{V}_2 = |\beta_2\rangle\langle\beta_2|. \quad (2.2)$$

This condition will give us a great advantage when we solve the dynamical equation.

The time-independent part of the potential is attractive while the time-dependent one is repulsive:

$$\lambda_1 < 0 \quad (2.3a)$$

$$\lambda_2(t) > 0 \quad \text{if } 0 < t < T \quad (2.3b)$$

$$\lambda_2(t) = 0 \quad \text{otherwise.}$$

Equation (2.3b) shows that at the beginning ( $t = 0$ ) the Hamiltonian contains only an attractive potential and there is a repulsive perturbation between the times zero and  $T$ .

The state of a particle moving in the potential is described by the Schrödinger equation

$$i \frac{\partial}{\partial t} |\Psi(t)\rangle = \hat{H}(t) |\Psi(t)\rangle. \quad (2.4)$$

The initial condition is

$$|\Psi(0)\rangle = |\phi_B\rangle \quad (2.5)$$

where  $|\phi_B\rangle$  is a bound state of  $\hat{H}(0) = \hat{H}_1$ :

$$\hat{H}_1 |\phi_B\rangle = E_B |\phi_B\rangle. \quad (2.6)$$

The value of  $\lambda_1$  will be chosen so that  $|\phi_B\rangle$  is the only bound state of  $\hat{H}_1$ . Then this bound state with the scattering states of  $\hat{H}_1$

$$\hat{H}_1 |\phi_{\mathbf{k}}^\pm\rangle = \mathbf{k}^2 |\phi_{\mathbf{k}}^\pm\rangle \quad (2.7)$$

form a complete and orthonormal set:

$$|\phi_B\rangle\langle\phi_B| + \int d\mathbf{k} |\phi_{\mathbf{k}}^\pm\rangle\langle\phi_{\mathbf{k}}^\pm| = \hat{1} \quad (2.8a)$$

$$\langle\phi_{\mathbf{k}}^\pm|\phi_{\mathbf{k}'}^\pm\rangle = \delta(\mathbf{k} - \mathbf{k}') \quad \langle\phi_{\mathbf{k}}^\pm|\phi_B\rangle = 0. \quad (2.8b)$$

The probability that the particle will be in the bound state after the perturbation (at  $t \rightarrow \infty$ ) is

$$w_B \equiv w_B(\infty) = w_B(T) = |\langle\phi_B|\Psi(T)\rangle|^2. \quad (2.9)$$

The probability of detecting the particle infinitely far from the potential region with momentum  $\mathbf{k}$  when  $t \rightarrow \infty$  is

$$w_{\mathbf{k}} \equiv w_{\mathbf{k}}(\infty) = w_{\mathbf{k}}(T) = |\langle\phi_{\mathbf{k}}^-|\Psi(T)\rangle|^2. \quad (2.10)$$

To calculate the probabilities  $w_B$  and  $w_{\mathbf{k}}$  one has to know the state  $|\Psi(T)\rangle$ .

† Note that  $\beta_i$  are not spatial variables;  $\langle\mathbf{r}|\beta_i\rangle = f(\mathbf{r}, \beta_i)$  is the function related to  $|\beta_i\rangle$  in  $\mathbf{r}$  representation where  $\mathbf{r}$  can be a spatial variable.

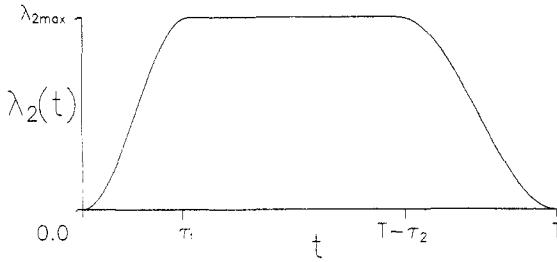


Figure 1. The time dependence of the strength of the repulsive part of the potential (5.1).

### 3. Solution

In this section we show how to calculate the state

$$|\Psi(T)\rangle = \hat{\Gamma}(T, 0)|\Psi(0)\rangle = \hat{\Gamma}(T, 0)|\phi_B\rangle \tag{3.1}$$

where

$$i \frac{\partial}{\partial t} \hat{\Gamma}(t, t') = \hat{H}(t) \hat{\Gamma}(t, t') \tag{3.2a}$$

$$i \frac{\partial}{\partial t'} \hat{\Gamma}(t, t') = -\hat{\Gamma}(t, t') \hat{H}(t') \tag{3.2a}$$

$$\hat{\Gamma}(t, t) = \hat{1}. \tag{3.2b}$$

$\hat{\Gamma}(t, t')$  is the time-evolution operator associated with  $\hat{H}(t)$ . It has the important property

$$\hat{\Gamma}(t, t') = \hat{\Gamma}(t, t'') \hat{\Gamma}(t'', t') \tag{3.3}$$

and also satisfies the following equation:

$$\hat{\Gamma}(t, t') = \hat{\Gamma}_1(t, t') - i \int_{t'}^t dt'' \hat{\Gamma}_1(t, t'') \hat{V}_2(t'') \hat{\Gamma}(t'', t') \tag{3.4a}$$

$$= \hat{\Gamma}_1(t, t') - i \int_{t'}^t dt'' \hat{\Gamma}(t, t'') \hat{V}_2(t'') \hat{\Gamma}_1(t'', t') \tag{3.4b}$$

where

$$\hat{\Gamma}_1(t, t') = e^{-i\hat{H}_1(t-t')} \tag{3.5}$$

is the time-evolution operator associated with the time-independent Hamiltonian  $\hat{H}_1$ .

Using equations (3.1) and (3.4a) one can obtain a Volterra-type integral equation for  $|\Psi(t)\rangle$ :

$$|\Psi(t)\rangle = \hat{\Gamma}_1(t, t') |\Psi(t')\rangle - i \int_{t'}^t dt'' \hat{\Gamma}_1(t, t'') \hat{V}_2(t'') |\Psi(t'')\rangle \tag{3.6}$$

where  $t' \leq t'' \leq t$ . For further specialization of the time dependence of the potential  $\hat{V}_2(t) = \lambda_2(t) \hat{V}_2$  we assume that  $\lambda_2(t)$  is a continuous and differentiable function which has a non-zero constant part. The length of the constant part of the potential is denoted by  $\tau$ , and  $\tau_1, \tau_2$  denote the switch-in and switch-off times of the potential, respectively. The meaning of the parameters of the function  $\lambda_2(t)$  can be seen in figure 1.

Taking into account (3.1), (3.3), (3.6) and the shape of the time dependence of the potential it is advantageous to write the state  $|\Psi(T)\rangle$  in the following form:

$$|\Psi(T)\rangle = \hat{\Gamma}(T, T - \tau_2)\hat{\Gamma}(T - \tau_2, \tau_1)\hat{\Gamma}(\tau_1, 0)|\phi_B\rangle \tag{3.7}$$

and to calculate  $|\Psi(T)\rangle$  in three steps. In the first step substituting  $t = \tau_1$  and  $t' = 0$  in (3.6) and using (3.5), (2.6) and (2.2) one arrives at

$$|\Psi(\tau_1)\rangle = e^{-iE_B\tau_1}|\phi_B\rangle - i \int_0^{\tau_1} dt'' \hat{\Gamma}_1(\tau_1, t'')|\beta_2\rangle x_2(t'') \tag{3.8}$$

where the notation

$$x_2(t) = \lambda_2(t)\langle\beta_2|\Psi(t)\rangle$$

has been introduced. On the other hand, multiplying (3.6) with  $\lambda_2(t)\langle\beta_2|$  from the left, in the case of  $0 < t < \tau_1$  and  $t' = 0$  we get a Volterra-type equation for  $x_2(t)$ :

$$x_2(t) = \lambda_2(t)\left\{ \langle\beta_2|\phi_B\rangle e^{-iE_B t} - i \int_0^t dt'' \langle\beta_2|\hat{\Gamma}_1(t, t'')|\beta_2\rangle x_2(t'') \right\}. \tag{3.9}$$

Since the Dirac brackets in (3.9) are known, this equation can be solved, at least numerically. (For further details, see [1].) If we know  $x_2(t)$ , we can calculate  $|\Psi(\tau_1)\rangle$ .

The following step is to calculate

$$|\Psi(T - \tau_2)\rangle = \hat{\Gamma}(T - \tau_2, \tau_1)|\Psi(\tau_1)\rangle. \tag{3.10}$$

In the interval  $(\tau_1, T - \tau_2)$   $\hat{H}$  is time independent. Therefore

$$\hat{\Gamma}(T - \tau_2, \tau_1) = e^{-i\hat{H}(T - \tau_2 - \tau_1)} = e^{-i\hat{H}\tau} \tag{3.11}$$

where

$$\hat{H} = \hat{H}_0 + \lambda_1 \hat{V}_1 + \lambda_{2max} \hat{V}_2. \tag{3.12}$$

The effect of the operator (3.11) on  $|\Psi(\tau_1)\rangle$  can be calculated so that one can find  $|\Psi(T - \tau_2)\rangle$ . We shall give a more detailed analysis of this calculation in the next section.

The last step consists in looking for

$$|\Psi(T)\rangle = \hat{\Gamma}(T, T - \tau_2)|\Psi(T - \tau_2)\rangle. \tag{3.13}$$

We use (3.6) again, substituting  $t = T$ ,  $t' = T - \tau_2$  and get

$$|\Psi(T)\rangle = \hat{\Gamma}_1(T, T - \tau_2)|\Psi(T - \tau_2)\rangle - i \int_{T - \tau_2}^T dt'' \hat{\Gamma}_1(T, t'')|\beta_2\rangle X_2(t''). \tag{3.14}$$

The definition of  $X_2(t)$  is formally the same as that of  $x_2(t)$  but  $X_2(t)$  is the solution of the following equation:

$$X_2(t) = \lambda_2(t)\left\{ \langle\beta_2|\hat{\Gamma}_1(t, T - \tau_2)|\Psi(T - \tau_2)\rangle - i \int_{T - \tau_2}^t dt'' \langle\beta_2|\hat{\Gamma}_1(t, t'')|\beta_2\rangle X_2(t'') \right\} \tag{3.15}$$

where  $T - \tau_2 < t < T$  and where the Dirac brackets are again known and the limits of integration differ from the earlier ones in (3.9). After one finds  $X_2(t)$ , it is possible to calculate the state  $|\Psi(T)\rangle$  from (3.14).

Note that using the fact that the potential is separable we obtained the equations (3.9) and (3.15), which are equations for complex functions with one variable instead of the dynamical equation (3.6), which is an operator equation with mixed spacetime variables and which may lead to an integrodifferential equation in the spacetime coordinates. Equations (3.8), (3.10) and (3.14) are exact equations for the time-dependent state. If (3.9) and (3.15) are solved numerically—which is generally the case—the method gives  $|\Psi(T)\rangle$  with arbitrary accuracy.

#### 4. The potential jump

In this section we shall consider the special case when the repulsive potential jumps up from zero to the value  $\lambda_{2\max} \hat{V}_2$  and then falls down to zero. Therefore now,  $\tau_1 = \tau_2 = 0$  and  $T = \tau$ . We have to calculate the matrix elements of the operator  $e^{-i\hat{H}\tau}$  in

$$w_B = |a_B|^2 = |\langle \phi_B | e^{-i\hat{H}\tau} | \phi_B \rangle|^2 \tag{4.1a}$$

$$w_k = |a_k|^2 = |\langle \phi_k^- | e^{-i\hat{H}\tau} | \phi_B \rangle|^2. \tag{4.1b}$$

To evaluate these expressions let us write the operator  $e^{-i\hat{H}\tau}$  in the form of a Fourier integral:

$$e^{-i\hat{H}\tau} = \frac{1}{2\pi} \int_{-\infty}^{+\infty} d\omega e^{-i\omega\tau} \hat{G}(\omega + i\epsilon) \tag{4.2}$$

where

$$\hat{G}(\omega) = (\omega - \hat{H})^{-1} \tag{4.3}$$

is the resolvent operator associated with  $\hat{H}$ . It is known from stationary scattering theory that the matrix elements of  $\hat{G}(\omega)$  appearing in (4.1) may be continued analytically into the complex  $\omega$  plane. This plane has two sheets; a physical and a non-physical sheet. There is a cut separating the two sheets along the positive real axis. The bound state poles lie on the negative real axis, and the resonance poles in the fourth quadrant of the non-physical sheet. Taking advantage of this analytical structure, we shall deform the path of integration in (4.2) because it is complicated to calculate the integral along the real axis. Using the residuum theorem we obtain

$$\int_{-\infty}^0 d\omega e^{-i\omega\tau} \hat{G}(\omega + i\epsilon) = \int_{-i\infty}^0 d\omega e^{-i\omega\tau} \hat{G}(\omega) - 2\pi i \text{res} \{e^{-i\omega\tau} \hat{G}(\omega); 3^\uparrow\}. \tag{4.4}$$

The term  $\text{res} \{e^{-i\omega\tau} \hat{G}(\omega); 3^\uparrow\}$  denotes the residua of the poles which are on the negative real axis or in the third quadrant of the physical sheet. In (4.4) we used the fact that the integral on the infinite circle in the lower half-plane vanishes because of the factor  $e^{-i\omega\tau}$ . Similarly

$$\int_0^{+\infty} d\omega e^{-i\omega\tau} \hat{G}(\omega + i\epsilon) = \int_0^{-i\infty} d\omega e^{-i\omega\tau} \hat{G}(\omega) - 2\pi i \text{res} \{e^{-i\omega\tau} \hat{G}(\omega); 4^\downarrow\} \tag{4.5}$$

where  $\text{res}\{e^{-i\omega\tau}\hat{G}(\omega); 4^\downarrow\}$  are the residua of the corresponding poles in the fourth quadrant of the non-physical sheet, including the positive real axis. We chose the parameters of the potentials so that  $\hat{H}$  has no bound states. This means that the matrix elements of  $\hat{G}(\omega)$  have no poles on the negative axis in the physical sheet. So  $\text{res}\{e^{-i\omega\tau}\hat{G}(\omega); 3^\uparrow\}$  equals zero.

Then adding (4.4) and (4.5)

$$e^{-i\hat{H}\tau} = -\frac{1}{2\pi} \left( \int_0^{-i\infty} d\omega e^{-i\omega\tau} \{\hat{G}^\uparrow(\omega) - \hat{G}^\downarrow(\omega)\} + 2\pi i \text{res}\{e^{-i\omega\tau}\hat{G}(\omega); 4^\downarrow\} \right). \tag{4.6}$$

The notations  $\hat{G}^\uparrow$  and  $\hat{G}^\downarrow$  have been introduced to make a difference between the values of  $\hat{G}$  in the different sheets of the plane  $\omega$ . Substituting  $\omega = -i\Omega$  in (4.6) we get

$$e^{-i\hat{H}\tau} = \frac{1}{2\pi} \left( i \int_0^{+\infty} d\Omega e^{-\Omega\tau} \{\hat{G}^\uparrow(-i\Omega) - \hat{G}^\downarrow(-i\Omega)\} - 2\pi i \text{res}\{e^{-i\omega\tau}\hat{G}(\omega); 4^\downarrow\} \right). \tag{4.7}$$

This expression shows that because of the factor  $e^{-\Omega\tau}$  the integrand decreases quickly if  $\tau$  is not very small. On the other hand, changing the integration variable  $\Omega \rightarrow \xi/\tau$

$$e^{-i\hat{H}\tau} = \frac{1}{2\pi} \left( \frac{i}{\tau} \int_0^{+\infty} d\xi e^{-\xi} \{\hat{G}^\uparrow(-i\xi/\tau) - \hat{G}^\downarrow(-i\xi/\tau)\} + 2\pi i \text{res}\{e^{-i\omega\tau}\hat{G}(\omega); 4^\downarrow\} \right). \tag{4.8}$$

The integral goes to zero when  $\tau$  goes to infinity. So, for  $\tau \rightarrow \infty$  the residua must go to a non-zero value in the case of  $w_{\mathbf{k}}$ , because  $w_{\mathbf{k}}$  is non-zero if  $\tau \rightarrow \infty$ . So if  $\tau$  is large then the integral is small, compared with the residua in the case of calculating  $w_{\mathbf{k}}$ . On the other hand, if  $\tau$  is large then the integral might be neglected in the case of  $w_{\mathbf{B}}$  if there is a pole far enough from the positive real axis. (Note that the amount of work of numerical calculation of the integral in (4.8) is independent of the value of  $\tau$ .) Using (4.8) one can write

$$a_{\mathbf{k}} = \frac{1}{2\pi} \left( \frac{i}{\tau} \int_0^{+\infty} d\xi e^{-\xi} \{ \langle \phi_{\mathbf{k}}^- | \hat{G}^\uparrow(-i\xi/\tau) - \hat{G}^\downarrow(-i\xi/\tau) | \phi_{\mathbf{B}} \rangle + \sum_j e^{-i\omega_j\tau} 2\pi i \text{res}\{ \langle \phi_{\mathbf{k}}^- | \hat{G}(\omega) | \phi_{\mathbf{B}} \rangle \}_{\omega=\omega_j} \right) \tag{4.9}$$

where  $\omega_j$  denotes the location of the  $j$ th pole belonging to the matrix elements of  $\hat{G}(\omega)$ . On the other hand using that  $\hat{V}_2$  is separable one can prove that

$$\hat{G}(\omega) = \hat{G}_1(\omega) + \hat{G}_1(\omega) |\beta_2\rangle \langle M^{-1}(\omega)_{22} \langle \beta_2 | \hat{G}_1(\omega) \tag{4.10}$$

where

$$\hat{G}_1(\omega) = (\omega - \hat{H}_1)^{-1} \tag{4.11}$$

is the resolvent operator of  $\hat{H}_1$  and

$$M_{ij}(\omega) = \frac{\delta_{ij}}{\lambda_j} - \langle \beta_i | \hat{G}_0(\omega) | \beta_j \rangle \quad (i, j = 1, 2) \tag{4.12}$$

where  $\hat{G}_0$  is the free Green operator. Using (4.10), (4.11) and taking into account (2.6) and (2.7) we get:

$$\langle \phi_{\mathbf{k}}^- | \hat{G}(\omega) | \phi_{\mathbf{B}} \rangle = \frac{\langle \phi_{\mathbf{k}}^- | \phi_{\mathbf{B}} \rangle}{\omega - E_{\mathbf{B}}} + \frac{\langle \phi_{\mathbf{k}}^- | \beta_2 \rangle}{\omega - \mathbf{k}^2} (M^{-1}(\omega))_{22} \frac{\langle \beta_2 | \phi_{\mathbf{B}} \rangle}{\omega - E_{\mathbf{B}}}. \quad (4.13)$$

The first term of (4.13) vanishes because of the orthogonality (2.8b). That is why it is sufficient to deal with the second term in (4.13). For simplicity, we take into account only one zero of  $\det M(\omega)$  at  $E_1 - \frac{1}{2}i\Gamma_1$ . Then one can write (see appendix A) that

$$(M^{-1}(\omega))_{22} = \frac{\omega - E_{\mathbf{B}}}{\omega - E_1 + \frac{1}{2}i\Gamma_1} f(\omega) \quad (4.14)$$

where  $f(\omega)$  is a regular function. So in the case of  $a_{\mathbf{k}}$ :

$$\text{residua} = \langle \phi_{\mathbf{k}}^- | \beta_2 \rangle \langle \beta_2 | \phi_{\mathbf{B}} \rangle e^{-i\mathbf{k}^2\tau} \frac{f(\mathbf{k}^2) - e^{-i(E_1 - \mathbf{k}^2)\tau} e^{-\Gamma_1\tau/2} f(E_1 - \frac{1}{2}i\Gamma_1)}{\mathbf{k}^2 - E_1 + \frac{1}{2}i\Gamma_1}. \quad (4.15)$$

Neglecting the integral term in (4.9) and taking the absolute square of (4.15) the interference term in  $w_{\mathbf{k}}$  is proportional to  $e^{-\Gamma_1\tau} \sin(\mathbf{k}^2 - E_1)\tau$ . These oscillations can be seen in the energy spectrum if  $\tau \approx \Gamma_1^{-1} \equiv \tau_{\text{life}}$ . If  $\tau \gg \tau_{\text{life}}$  the oscillations die out. If  $\tau \rightarrow \infty$  the integral in (4.9) and the term in (4.15), which is proportional to  $e^{-\Gamma_1\tau/2}$ , goes to zero, so we get the well known Lorentz spectrum. In the case of calculating  $a_{\mathbf{B}}$  one has to substitute  $E_{\mathbf{B}}$  for  $\mathbf{k}^2$  and  $|\phi_{\mathbf{B}}\rangle$  for  $|\Psi_{\mathbf{k}}^-\rangle$  in (4.13).

In this case the expression (4.13) has no singularity at  $\omega = E_{\mathbf{B}}$  (for details see appendix B) and after carrying out the integration the first term gives zero. So the first term of (4.13) vanishes again. Then the residue is proportional to  $e^{-\Gamma_1\tau}$ :

$$a_{\mathbf{B}} = |\langle \phi_{\mathbf{B}} | \beta_2 \rangle|^2 \frac{e^{-\Gamma_1\tau} e^{-iE_1\tau}}{E_1 - \frac{1}{2}i\Gamma_1 - E_{\mathbf{B}}} f(E_1 - \frac{1}{2}i\Gamma_1) + \text{integral}. \quad (4.16)$$

This formula shows that if the first term dominates then the decay is exponential. This is the situation when  $\tau \approx \tau_{\text{life}}$ . For  $\tau \rightarrow \infty$  the integral term dominates (the residue term is proportional to  $e^{-\Gamma_1\tau}$ ) and  $a_{\mathbf{B}} \sim \tau^{-3/2}$ , which is a deviation from the exponential law. (It can be proved that the integrand in (4.8) is proportional to  $\tau^{-1/2}$  when  $\tau$  goes to infinity.) Formulae from (4.2) to (4.8) and (4.10)–(4.12) are valid also in the general case when  $\tau_1$  and  $\tau_2$  are non-zero and  $T \neq \tau$ . Then the operator  $\hat{G}(\omega)$  should be calculated between states more complicated than  $|\phi_{\mathbf{B}}\rangle$  and  $|\phi_{\mathbf{k}}^-\rangle$ . The evolution of the wavefunction during the time intervals  $\tau_1$  and  $\tau_2$ , when the potential is explicitly time dependent, can be followed only numerically. The relevant results will be presented in the next section.



## 5. Numerical results

### 5.1. Specialization of the potential

In this section we shall show that with the aid of the model derived above one can study the relations between the parameters of the potential and the probabilities  $w_B$  and  $w_k$ . In subsection 5.4 we shall compare the model with an approximate method.

We chose the following time dependence for the potential  $\hat{V}_2(t) = \lambda_2(t)\hat{V}_2$ :

$$\lambda_2(t) = \begin{cases} \lambda_{2\max} \sin^2(t\pi/2\tau_1) & \text{if } 0 < t \leq \tau_1 \\ \lambda_{2\max} & \text{if } \tau_1 < t \leq T - \tau_2 \\ \lambda_{2\max} \sin^2[(t - T)\pi/2\tau_2] & \text{if } T - \tau_2 < t \leq T \\ 0 & \text{otherwise.} \end{cases} \quad (5.1)$$

The form factors of the potentials were *s*-wave Gaussians:

$$\langle k|\beta_j\rangle = \left(\frac{\beta_j}{\sqrt{\pi}}\right)^{3/2} \exp(-\frac{1}{2}k^2\beta_j^2). \quad (5.2)$$

This choice made the analytic evaluation of all the necessary matrix elements possible. The range  $\beta_1$  of the attraction was chosen to be a unit in an arbitrary dimensionless scale. With this choice we fixed the scale of distances and also of the energy in a dimensionless scale ( $\hbar = 1$ ,  $2m = 1$ ). The strength  $\lambda_1$  of the stationary potential was fixed to give  $E_B = -0.49$ .

Numerical experiences show that it is enough to take into account two poles throughout the calculations. These poles are moving in the  $\omega$  plane while the potential is changing. In the beginning, one of the poles is on the negative real axis in the physical sheet and the other is in the fourth quadrant of the non-physical one, relatively far from the real axis. When the repulsion is maximal, the two poles are at their turning points  $E_j - \frac{1}{2}i\Gamma_j$  ( $j = 1, 2$ ) in the non-physical sheet. If the pole which came from the lower part of the plane does not approach the first one—which is relatively near to the positive real axis—then it is enough to take into account the residuum belonging to the pole which is associated with the decaying bound state. During the application of the model we shall mainly deal with such cases.

Then we chose the range  $\beta_2$  of the repulsion controlling the distance of the turning point of the pole corresponding to the starting bound state from the positive  $\omega$  axis†.

Accordingly we had three different cases of resonance:

the 'broad' case:  $\Gamma_1 = 1.19$ ,  $E_1 = 0.84$  when  $\beta_2 = 2.0$  and  $\lambda_{2\max} = 1.6$

the 'normal' case:  $\Gamma_1 = 0.12$ ,  $E_1 = 0.80$  when  $\beta_2 = 1.8$  and  $\lambda_{2\max} = 1.4$

the 'narrow' case:  $\Gamma_1 = 0.011$ ,  $E_1 = 0.63$  when  $\beta_2 = 1.6$  and  $\lambda_{2\max} = 1.12$ .

The maximal strength  $\lambda_{2\max}$  of the repulsion controlled the distance from the other pole. The paths of the poles while  $0 < t < \tau_1$  or  $T - \tau_2 < t < T$ , and its position while  $\tau_1 < t < T - \tau_2$  can be seen in figure 2. One can see that in the 'broad' case the other pole approaches the first one and will have an effect on the probabilities  $w_B$  and  $w_k$ .

† We remark that in *s*-states the 'bound-state-pole' goes from the negative real axis of the physical sheet onto the negative real axis of the non-physical sheet while the repulsion grows. Then the pole sinks into the third quadrant of the non-physical sheet and goes over to the fourth quadrant. The location of the point where the pole leaves the axis and the distance from the axis in the fourth quadrant of the non-physical sheet is related to  $\beta_2$ .

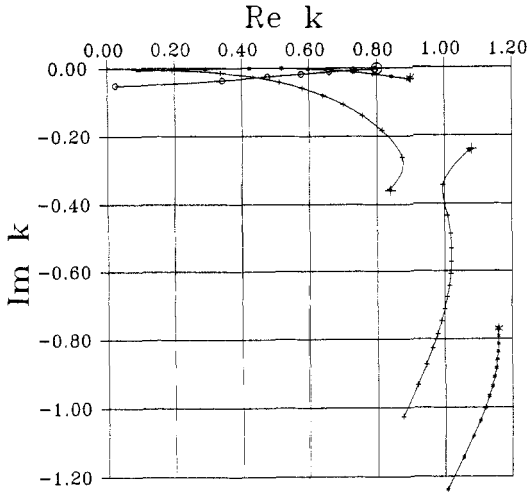


**Figure 2.** The paths of the poles associated to the three different cases of resonances in the plane  $k = \sqrt{\omega}$ . +, 'broad' case; \*, 'normal' case; O, 'narrow' case. (see section 5.1). The path of the second pole of the 'narrow' case is absent because that lies very far from the axes. At the points marked by large symbols (+, \*, O)  $\lambda_2 = \lambda_{2 \max}$ . (The step of  $\lambda_2$  is 0.1.)

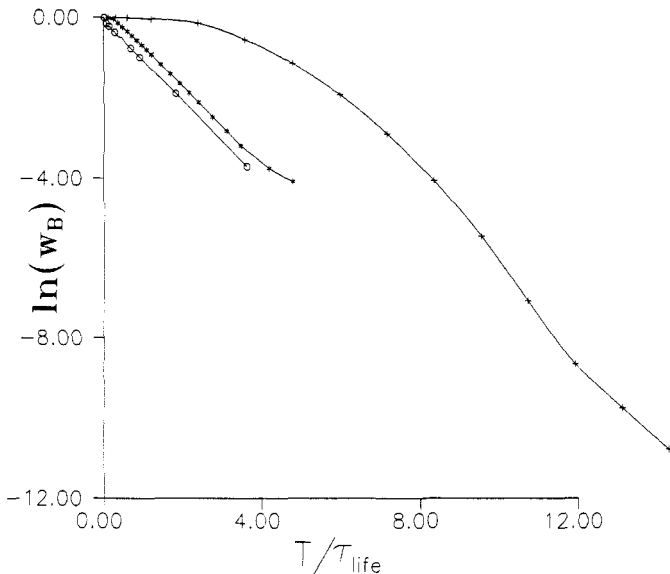


**Figure 3.** The time dependence of the decay in the three different cases of resonances. +, 'broad' case; \*, 'normal' case; O, 'narrow' case ( $w_B$  is defined by (2.9)).

### 5.2. Decay of the bound state

In the first application we study the exponential decay law. This is a typical one-pole rule which is valid in the case of the decay of a quasistationary state. The illustration of this can be seen in figure 3. In the 'broad' case—when the second pole gets close to the first one—the decay is not exponential. In the 'normal' and 'narrow' cases

we can say the following. As was seen from (4.16)  $w_B$  is proportional to  $e^{-\Gamma_1\tau}$  if  $\tau$  is around several times  $\tau_{\text{life}}$ . This property coming from the operator  $e^{-i\hat{H}\tau}$  holds even if  $\tau_1$  and  $\tau_2$  are non-zero. Results of this type are shown by the straight lines of figure 3. In the 'normal' case at large values of  $\tau$  one can see a deviation from the exponential. Numerical experiences show that even if  $\tau = 0$  while  $\tau_1 + \tau_2 \approx \tau_{\text{life}}$  the decay is exponential.

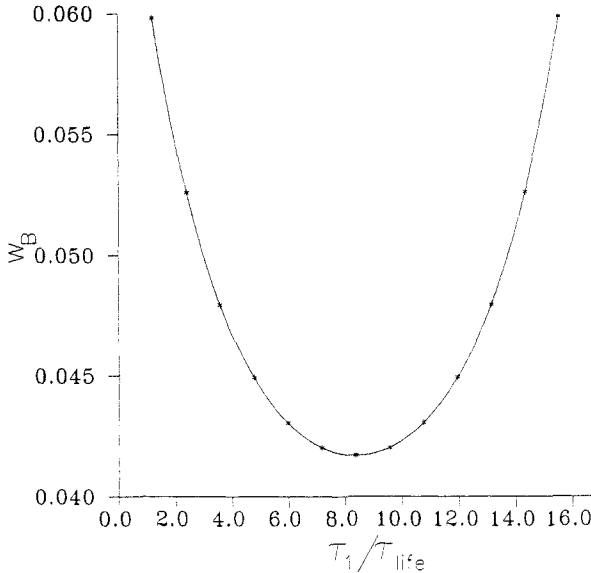
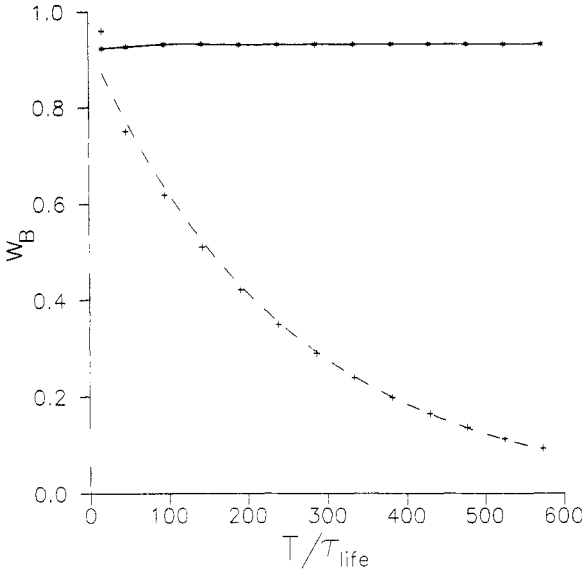


Figure 4. The dependence of the decay on the switch-times when  $\tau = 0$  and  $(\tau_1 + \tau_2)/\tau_{\text{life}} = 16.5 = \text{constant}$  (normal case,  $\tau_{\text{life}} \equiv \Gamma_1^{-1}$ ).

In the case of  $\tau \ll \tau_{\text{life}}$  the transients play a significant role. It is surprising that if  $\tau \ll \tau_{\text{life}}$  the value of  $w_B$  as a function of  $\tau$  is not even monotonous.

Our model gives the possibility to study the dependence of  $w_B$  and  $w_h$  on the switch-times  $\tau_1$  and  $\tau_2$ . So we chose  $\tau = 0$  and  $\tau_1 + \tau_2 = T = \text{constant}$ . The results are shown in figure 4. We see that if  $\tau_1 = \tau_2$ , the probability of staying in the bound state is the least. So, the time-symmetric perturbation disturbs the system the most. A further result is that  $w_B$  seems to depend only on the combination  $|\tau_1 - \tau_2|$  of the parameters  $\tau_1$  and  $\tau_2$  if  $\tau = 0$ . Also, the fast rise of the potential results in more particles coming out with high energy from the potential region. So the switch-in time seems to be important from the point of view of the spectrum.

It is possible to study the critical states in the model. We call a level critical if the associated energy is zero. If the (real part of the) energy of the level is a bit under or above zero then the level is called sub- or supercritical, respectively. (We remark that according to Zeldovich near the critical state the Dirac equation is related to a non-relativistic, local well-barrier potential [2].) Simulating a subcritical state we chose the parameter  $\lambda_{2\text{max}}$  so that the bound-state level got close to the zero value. The level spent  $\tau$  time in the subcritical state and then went back to the starting energy. In the supercritical case the level surpassed the zero by a small value. The probability  $w_B$  was calculated for different values of  $\tau$  ( $\tau_1 = \tau_2 = \text{constant}$ ). The results are in figure 5. It is clearly shown that particles decay from the supercritical



**Figure 5.** The time dependence of the decay from subcritical (\*) and supercritical (+) states. The broken curve indicates exponential fitting.

level almost exponentially, but practically they stay at the subcritical level. The small decay rate in the subcritical case is due to the non-zero speed of the changing of  $\hat{V}_2(t)$  in time.

### 5.3. The energy spectrum

The spectra associated with the the three types of resonances differ from each other. The most special feature of the spectra of the ‘normal’ and ‘narrow’ cases are the oscillations (see figure 6). For  $\tau_1 = \tau_2 = 0$  (i.e. the jump case) we have already shown the presence of the oscillations in section 4. The numerical results show that if  $\tau_1 \approx \tau_2 \ll \tau$  (i.e. a jump situation) then the period of the oscillation of the energy spectrum is around  $\tau \approx T = \tau + \tau_1 + \tau_2$ . If  $\tau \approx \tau_1 \approx \tau_2$  then the frequency is between  $\tau$  and  $T$ . There are oscillations in the spectrum if  $\tau \ll \tau_1, \tau_2$  and even if  $\tau = 0$ .

It is interesting to follow how a stationary spectrum develops while  $\tau$  is growing. If we imagine the time-development of the spectrum as a movie picture we see the following. Even at an extra short perturbation ( $w_B > 0.999$ ) the spectrum is not monotonous in any of the cases. There are several peaks going towards the ‘main’ one in time. By main we mean the peak which will develop into the stationary Lorentz-like peak at  $\tau = +\infty$ . The ‘main’ peak itself is moving from left to right, too, towards its final ( $\tau = +\infty$ ) location in the energy spectrum. This ‘main’ peak grows taller and slimmer in time. Meanwhile the other peaks turn into oscillations with decreasing wavelength and amplitude. The oscillations advances toward the ‘main’ peak both from low and high energies until they die out. At very large values of  $\tau$  ( $w_B \ll 10^{-3}$ ) the spectrum is a well known smooth Lorentzian curve or the superposition of several of them. These features are effective in the ‘normal’ and in the ‘narrow’ cases for all studied values of the switch parameters.

Our separable potential model has some special characteristics. One of these is that there exists a certain value of  $k$  where  $w_k = 0$  because  $\langle \phi_k^- | \beta_2 \rangle = 0$ . This is due

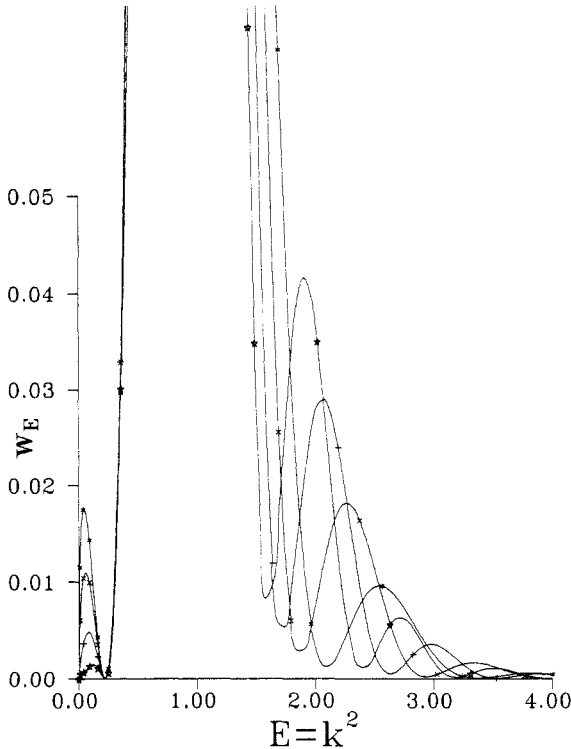


**Figure 6.** The typical oscillations of the spectra of the 'normal' and 'narrow' cases ( $\tau < \tau_{\text{life}}$ ,  $\omega_E = 2\pi k \omega_k$ ,  $\omega_k$  is defined by (2.10)).

to the form factor (5.2) used through the calculations. The location of this zero-point depends on the value of  $\beta_2$ . As  $\beta_2$  increases the zero-point of the spectrum goes toward the point  $E = k^2 = 0$  and around the value  $\beta_2 = 1.9$  it goes over to negative values which are not detectable in the spectrum. That is why in the 'broad' case ( $\beta_2 = 2.0$ ) one cannot observe such a point in the spectrum.

#### 5.4. Test of an approximate method

In this section we examine the accuracy of a 'moving-pole approximation' of [3]. The authors set out from the fact that a pole under the real  $\omega$  axis is associated with a resonant state which is related with a Lorentz-like spectrum. They substitute the moving pole by a set of stationary poles acting at different times. So the spectrum belonging to this kind of poles is a time-average of stationary Lorentz curves:

$$W_k = \frac{2}{\pi} \int_0^T dt \frac{\Gamma^2(t) W_B(t)}{(E(t) - k^2)^2 + \Gamma^2(t)}. \quad (5.3)$$

Here  $E(t)$  and  $\Gamma(t)$  give the path of the pole in the  $\omega$  plane and  $W_B(t)$  is the probability of staying in the resonant state. Taking into account that the decay is exponential in the case of one pole we receive an equation for  $W_B(t)$ :

$$i \frac{\partial}{\partial t} W_B(t) = -2\Gamma(t) W_B(t). \quad (5.4)$$

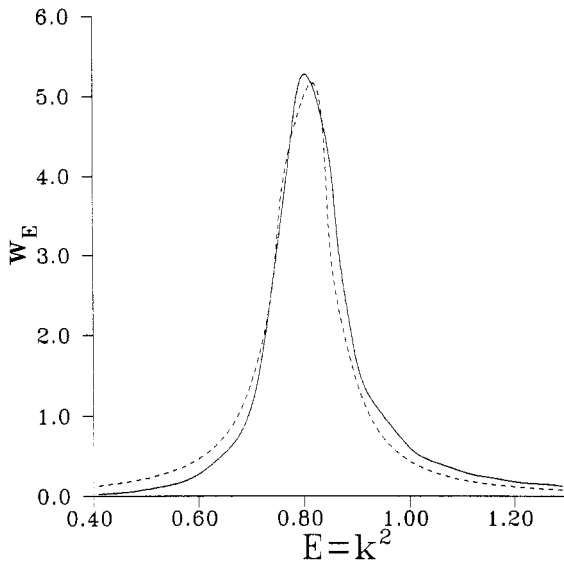


**Figure 7.** Comparison of the approximate formula (5.3) with the exact result in the 'normal' case for  $\tau \gg \tau_{\text{life}}$ . The full curve is the exact result,  $w_k$  in (2.10), and the broken curve is the approximate formula,  $W_k$  in (5.3);  $w_E = 2\pi k w_k$ .

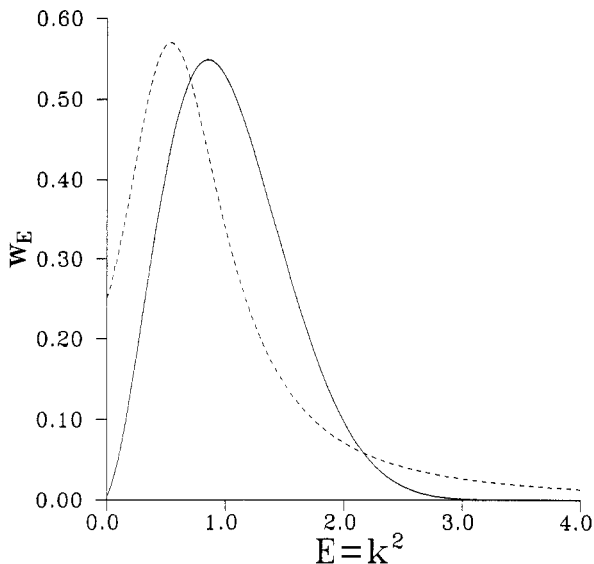


**Figure 8.** The effect of the second pole on the spectrum in the 'broad' case. The full curve is the exact result,  $w_k$  in (2.10), and the broken curve is the approximate formula,  $W_k$  in (5.3);  $w_E = 2\pi k w_k$ .

Now we examine the validity of the above approximation.

We expect that (5.3) is a good approximation both in the 'normal' and the 'narrow' cases in the jump situation if  $\tau \gg \tau_{\text{life}}$  (figure 7), because in the jump case the formula (5.3) is proportional to the exact one if  $T \gg \tau_{\text{life}}$ . If  $T \ll \tau_{\text{life}}$  (5.3) is not a good

approximation because the integral term of the exact amplitude has not yet died.

In the 'broad' case, for  $\lambda_{2\max} = 1.6$ , the one-pole approximation fails as we have seen earlier. In this case, decreasing  $\lambda_{2\max}$ , we could study when the one pole approximation can be applied at all. As we decreased the value of  $\lambda_{2\max}$  both the distance between the turning points of the two poles and the distance between the real  $\omega$  axis and the turning point of the second pole increased. So the effect of the second pole on the spectrum decreased. One can see the typical effect of the second pole on the spectrum in figure 8.

## Appendix A

By definition

$$(M^{-1}(\omega))_{22} = \frac{M_{11}(\omega)}{\det M(\omega)}. \quad (\text{A.1})$$

The definition of  $M_{11}(\omega)$  can be found in (4.12). On the other hand, from (2.6) it follows that

$$|\phi_B\rangle = \hat{G}_0(E_B)\lambda_1\hat{V}_1|\phi_B\rangle. \quad (\text{A.2})$$

Multiplying by  $\langle\beta_1|$  and using (2.2) and that  $\langle\beta_1|\phi_B\rangle \neq 0$ , one obtains

$$\frac{1}{\lambda_1} = \langle\beta_1|\hat{G}_0(E_B)|\beta_1\rangle. \quad (\text{A.3})$$

Substituting (A.3) into the definition of  $M_{11}(\omega)$  and doing algebraic steps one can obtain

$$M_{11}(\omega) = (\omega - E_B)\langle\beta_1|\hat{G}_0(\omega)\hat{G}_0(E_B)|\beta_1\rangle. \quad (\text{A.4})$$

According to (4.13) the resonance pole of  $\hat{G}(\omega)$  must correspond to a singularity of  $M^{-1}(\omega)$ , that is

$$\det M(\omega) = (\omega - E_1 + \frac{1}{2}i\Gamma_1)g(\omega) \quad (\text{A.5})$$

where  $g(\omega)$  is a regular function (taking into account only one resonance). Substituting (A.4) and (A.5) in (A.1) we get (4.14) where  $f(\omega) = \langle\beta_1|\hat{G}_0(\omega)\hat{G}_0(E_B)|\beta_1\rangle/g(\omega)$ .

## Appendix B

In calculating  $a_B$  one has to evaluate

$$\langle\phi_B|\hat{G}(\omega)|\phi_B\rangle = \frac{1}{\omega - E_B} \left[ 1 + \frac{|\langle\phi_B|\beta_2\rangle|^2}{\omega - E_B} (M^{-1}(\omega))_{22} \right]. \quad (\text{B.1})$$

Using (A.1), (A.4), (4.12) and that  $|\phi_B\rangle = \hat{G}_0(E_B)|\beta_1\rangle\langle\beta_1|\hat{G}_0^2(E_B)|\beta_1\rangle^{-1/2}$ , we obtain, after algebraic steps,

$$\begin{aligned} \langle\phi_B|\hat{G}(\omega)|\phi_B\rangle &= \frac{\langle\beta_1|\hat{G}_0(\omega)\hat{G}_0(E_B)|\beta_1\rangle M_{22}(\omega)}{\det M(\omega)} \\ &+ \frac{\langle\beta_1|\hat{G}_0(E_B)(\hat{G}_0(\omega) - \hat{G}_0(E_B))|\beta_1\rangle M_{12}^2(\omega)}{\det M(\omega)(\omega - E_B)\langle\beta_1|\hat{G}_0^2(E_B)|\beta_1\rangle}. \end{aligned} \quad (\text{B.2})$$

The first term of (B.2) is finite if  $\omega \rightarrow E_B$ .

With  $\hat{G}_0(\omega) - \hat{G}_0(E_B) = -(\omega - E_B)\hat{G}_0(\omega)\hat{G}_0(E_B)$ , the second term becomes

$$\frac{\langle\beta_1|\hat{G}_0(\omega)\hat{G}_0(E_B) - \hat{G}_0^2(E_B)|\beta_1\rangle M_{12}^2(\omega)}{\det M(\omega)(\omega - E_B)\langle\beta_1|\hat{G}_0^2(E_B)|\beta_1\rangle} = \frac{\langle\beta_1|\hat{G}_0(\omega)\hat{G}_0^2(E_B)|\beta_1\rangle M_{12}^2(\omega)}{\det M(\omega)\langle\beta_1|\hat{G}_0^2(E_B)|\beta_1\rangle} \quad (\text{B.3})$$

which is also finite for  $\omega \rightarrow E_B$ .

### Acknowledgments

The author is grateful to J Révai and A Frenkel for numerous fruitful discussions.

### References

- [1] Révai J 1988 Model for studying time-dependent quantum mechanical processes and its application for quasi-stationary states *Report KFKI-1988-57/A* Hungarian Academy of Sciences, Budapest
- [2] Zeldowich Ya B and Popov V S 1971 *Usp. Fiz. Nauk.* 105 403
- [3] Milek B and Reif R 1986 *Nucl. Phys. A* 458 366